Metrol. Meas. Syst., Vol. 28 (2021) No. 4, pp. 609–626
DOI: 10.24425/mms.2021.137699

PAN POLSKA AKADEMIA NAUK

METROLOGY AND MEASUREMENT SYSTEMS

Index 330930, ISSN 0860-8229
www.metrology.wat.edu.pl

M&MS

IMPROVED CALIBRATION UNCERTAINTY ASSESSMENT TECHNIQUE IN COORDINATE METROLOGY CONSIDERING THERMAL INFLUENCES

Meirbek Mussatayev[1)], Meifa Huang[1)], Marat Nurtas[2)], Azamat Arynov[3)]

1) *Guilin University of Electronic Technology, School of Mechanical & Electrical Engineering, 1 Jinji Rd, Guilin, Guangxi, 541004, China* (*mussatayevm@gmail.com*, ✉ *hmfzyr@hotmail.com*, +8 613 977 329 358)
2) *International Information Technology University, Department of Mathematical and Computer Modelling, Kazakhstan* (*maratnurtas@gmail.com*)
3) *School of Engineering at Warwick University, United Kingdom* (*azamat.arynov@warwick.ac.uk*)

Abstract

Reliable measurement uncertainty is a crucial part of the conformance/nonconformance decision-making process in the field of Quality Control in Manufacturing. The conventional GUM-method cannot be applied to CMM measurements primarily because of lack of an analytical relationship between the input quantities and the measurement. This paper presents calibration uncertainty analysis in commercial CMM-based Coordinate Metrology. For the case study, the hole-plate calibrated by the PTB is used as a workpiece. The paper focuses on thermo-mechanical errors which immediately affect the dimensional accuracy of manufactured parts of high-precision manufacturers. Our findings have highlighted some practical issues related to the importance of maintaining thermal equilibrium before the measurement. The authors have concluded that the thermal influence as an uncertainty contributor of CMM measurement result dominates the overall budgets for this example. The improved calibration uncertainty assessment technique considering thermal influence is described in detail for the use of a wide range of CMM users.

Keywords: coordinate measuring machine, coordinate metrology, uncertainty, quality control, thermal influence.

1. Introduction

Nowadays the competition among the producers requires them to not only produce low cost products, but also maintain a high performance level. *Coordinate Measuring Machines* (CMM) are currently broadly used in the manufacturing industry to meet that demand. A CMM is a measuring system used to measure the physical geometrical parameters of an object, and a CMM is perfectly tailored to the need for inspection control, which is growing rapidly. The main reason for this is driven by the fact that our global world is at the start of a new industrial revolution.

High quality inspection performance is one of the major factors of evaluating the quality of products in manufacturing. Single inspection tasks of a product are performed with commonly

Article history: received February 17, 2021; revised June 23, 2021; accepted June 25, 2021; available online July 4, 2021.

used (1D) inspection measurement instruments, such as Vernier calipers, screw micrometers and others. For more complex inspection tasks, *e.g.* geometrical tolerances or repetitive measurements, conventional CMMs are used. The ISO 10360-2 [1] standard requires that all decisions regarding conformance to specifications follow the rules listed in [2].

The main point of inspection is primarily related to ensuring compliance with the tolerance requirements of dimensional properties. On the one hand every measurement is only an estimate of the true value, on the other hand, uncertainty, according to standardized rules, identifies where the true value of measurement result is within a certain range [3].

We have already witnessed that the ISO 14253 [2] standard provides clear guidance about the necessity in allowing for the accuracy of the measuring instrument by reducing the size of the acceptance band. However, the main problem arises when a measurement result falls close to the upper or lower specification limit. The latter case with various examples is explained in detail in reference [4]. Thus, there is considerable interest in having access to measurement instruments with better accuracy – unfortunately these are usually more expensive to purchase, and may involve additional expenses such as special air-conditioned rooms or a longer measuring period [5].

It is well known that Part 1 of the ISO 15530 standard [6] provides clear uncertainty evaluation methods for sensitivity analysis [7], use of calibrated artefacts [8] as well as those for users of *Virtual Coordinate Measuring Machines* (VCMM) [9–11]. Practically, the best method for estimating measurement uncertainty is the one based on the use of calibrated artefacts described in [11, 12]. However, if a material standard is used at other temperatures, the calibration and the verification are not necessarily valid, and additional error is present due to unknown *thermal expansion coefficient* (CTE). Consequently, this increases the total uncertainty budget [13]. The outcome of our research contained in the teams' last paper [8] clearly stated that the expanded uncertainty in the low industrial conditions was double that of the improved industrial conditions in the total uncertainty budget of the given study. Finally, because CMMs are installed on a typical shop floor, environmental temperatures may vary. In the experimental part of this research, only some major points were examined in order to pay special attention to thermal influences. It should be noted that the definition of error in this research was based on the measurement difference between a known value from the PTB (*Physikalisch-Technische Bundesanstalt* – the National Metrology Institute of Germany) and a measured value from a CMM. A similar approach is presented in the standard [14], where the uncertainty being evaluated only quantifies how accurate the test is. In comparison with our task specific uncertainty, the test uncertainty described in the standard [14] is only an indication of the quality of the test, and not an evaluation of CMM performance.

A similar uncertainty assessment approach for time-varying temperature environment can be found [15]. However, it is inherently not suitable for easing up the calculation method and still has not been implemented in measurements of calibration uncertainty for a variety of workpieces. In [16] there is presented an uncertainty evaluation model (distance between a point and a plane defined by 3 points) which enables uncertainty evaluation for different measuring tasks. The limitation of this approach is that the uncertainty assessment technique would only be applicable to estimating the discussed cases of position and out-of-plane parallelism of axes. In [17] the authors perform an analysis of various elements to be considered in the implementation uncertainty of circular features. Another research was conducted [18] to compare two uncertainty combined methods based on *Guide to the Expression of Uncertainty in Measurement* (GUM) with the Monte Carlo method. The feasibility of the evaluation method has been verified by the measurement example of flatness. The conducted experiments show that precision significance of uncertainty determined by the GUM is unreliable as the expanded uncertainty increased by 11.1% compared

Metrol. Meas. Syst., Vol. 28 (2021), No. 4, pp. 609–626
DOI: 10.24425/mms.2021.137699

to the actual results. The paper [7] shows an application of the sensitivity approach to evaluation of measurement uncertainty of straightness, coaxiality, concentricity, position of axis, runout and distance between axes. Task specific uncertainty assessment techniques are still up-to-date and investigated by researchers [19–21]. However, only several uncertainty assessment techniques are available for the specific points of the calibration of CMMs, including those mentioned above. In practice, the problem of temperature induced errors for advanced measuring systems is primary concern. Particularly, the measurement results obtained with a displacement laser interferometer which are used for the calibration of the CMMs were corrected to 20°C [22]. Frequently missed in uncertainty budgets for alignment measurements, thermal errors and the uncertainty of any compensations applied can be critical for high precision alignment. Thus, for high precision applications, not only accurate alignment metrology is important but also precision compensation effects [23].

The objective of this research was to carry out a calibration procedure of a CMM and to present a more sophisticated assessment technique to improve the results of the former research. We emphasized the importance of temperature induced uncertainty and many of the situations where consideration of it would be most useful, such as:

a) non-20°C temperature CMM error as an uncertainty contributor,
b) machine repeatability and reproducibility,
c) temporal thermal gradients,
d) sampling strategies, *i.e.* the number and location of points in the workpiece coordinate system.

2. Presentation of the problem and the chosen solution approach

In practice, the error induced due to thermal influences causes CMM components to expand and bend. This error has a complex non-linear nature, which is why it is quite difficult to handle. Some of the contributing to the development of thermal errors are a) the distribution of the temperature of a CMM influenced by external sources, b) the gradient of the temperature, c) uniform temperature changes, and d) the material of a machine component and its thermal properties.

The accuracies of a machine are usually presented in the specifications of the producer. However, these accuracies are tested for the laboratory environment. Therefore, it should be noted that for CMMs installed in an environment in which the temperature is not well controlled, the accuracies might be lower. By dividing our experiment for the LIC (an environment in which the temperature was not well controlled) and improved industrial conditions (a laboratory environment), we attempted to estimate how the machine accuracy changed in varying temperatures. The experimental part of the research at the initial stage could be performed as a set of measurements using a CMM under various temperature conditions. In fact, the working time of the machine had to be constantly altered in order to better understand the influence of the heat dissipation of the CMM components on the measurement results [24].

Initially, we discussed in a review paper [25] the importance of the uncertainty of measurement using CMMs in the manufacturing industry. In a previous study [8], the state-of-the-art technique for the assessment of uncertainty was described in detail. A case study of the hole distance measurement from 50 mm to 750 mm was used. The measurement results showed that the uncertainty under the *improved industrial conditions* (IIC) was much higher compared to the *low industrial conditions* (LIC) (the terminology borrowed from ISO 230-9 [26]). Consequently, the thermal influence as an uncertainty component was the most significant contributor to the

last study. Since this paper describes the examination of the effect of thermal fluctuations on the uncertainty of CMM calibration, which are commonly used instruments, it will be of interest to readers in the field of manufacturing.

3. Case study

3.1. Calibration object

For our case study the accuracy of the CMMs was tested with a hole-plate. We had chosen the hole plate with 52 holes which is shown in Fig. 1(b) because it can be approached from both sides and tends to be lighter than a ball plate of similar size. The serial number of the object was PTB 5.32-95/5. The calibration object was made of grey cast iron ($\alpha \approx 10.5 \times 10^{-6^\circ}\mathrm{C}^{-1}$). The relative locations of cylindrical holes contained in a common plane were highly adapted for the verification of the CMMs. It should be noted that an artifact should be measured with di?erent orientations and locations in the CMM measurement range. This allows the estimation of the CMM accuracy of length measurement. This method is time- and cost-effective compared to the use of lasers. The calibration process was performed without compensation in order to compare our case study results with the calibration certificate of the PTB for the same hole-plate.

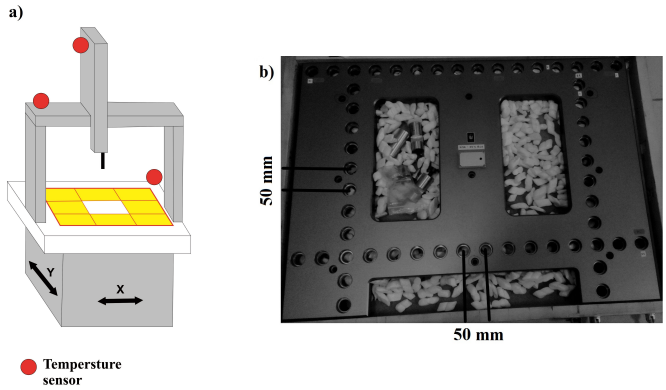

Fig. 1. (a) The location of temperature sensors. (b) A hole-plate with sample point numbers and distance between them (adapted from [8]).

A hole-plate standard was used as a workpiece to investigate the effect of thermal influences on the accuracy of the CMM. Next, based on the obtained results, the estimation of the measurement uncertainty of distance between two holes was performed. Therefore, we could experimentally determine whether the thermal influences of the most important uncertainty contributed. A method for quantifying the influence of the thermal deviations on the measurement uncertainty was also elaborated upon. Finally, some results illustrated how this method could be useful in practice.

The experiments were performed with the use of a high accuracy machine, DEA GLOBAL Silver CMM (with touch-trigger TESASTAR probes and High-Speed-Scanning Leitz sensors) manufactured by Hexagon MI. The sensor type was chosen based on the application. The main machine properties were a) work volume: $1000 \times 700 \times 660$ mm^3, and b) specified maximum permissible error of indication for size measurements: $\mathrm{E}_{0,MPE} = \pm(1.4+L/333)\mu$m at $(20\pm1)^\circ$C, with length L under measurement in mms. The conducted measurement process is illustrated in Fig. 2.

Metrol. Meas. Syst., Vol. 28 (2021), No. 4, pp. 609–626
DOI: 10.24425/mms.2021.137699

Fig. 2. Coordinate measurement process to obtain geometric measurements.

The measurements began with the determination of the coordinate system of the workpiece. Each hole was measured three times, and repeated runs were averaged to improve the coordinate accuracy. Each hole was measured in three cross-sections using three points to precisely identify the midpoint of each hole. Repeated points were used to check the repeatability of the system. This allowed any drift in the machine coordinate system to be measured as well.

In practice, for each hole, one measurement took more than 1 minute. Consequently, for the 52 holes, it took more than 1 hour for one complete measurement. The hole-plate was measured more than fifteen times, with five repeated measurements under each environmental conditions. Moreover, one measurement was carried out in one orientation, and another measurement was carried out after rotating the plate by 180°.

3.2. Measurement conditions

An appropriate environmental condition is one of the key factors for experimentation because the effects of environmental changes on machine accuracy are highly important. Air temperature, pressure, humidity, and vibration all influence the length scales of a machine. Hence, it is recommended that a CMM environment should be in line with high settings, representing "improved working conditions" [10]. In this research, while the highest quality grid plates were made from materials which had small CTE, the machine was made of steel. In addition, in order to maintain the room temperature at a nearly constant level, as many heat sources as possible were controlled.

For instance

a) the room had indirect lighting to prevent shadows;
b) the measurement was completely automated so that no human heat source needed to be present near the machine after the run began;
c) thermocouples were placed at each axis on the machine as Fig. 1(b) illustrates. They were used to measure the thermal profile of the machine as the experimental measurements are made to check on the actual thermal stability of the machine frame;
d) generally, the machine was run through a warm-up cycle to assure that the thermal equilibrium was reached before the measurement run began.

The environmental condition in the room was quite good over long periods of time, within 0.2°C, but since the room was not separately thermostated, occasional temperature excursions might occur. A human heat source might create a negative effect on the air temperature within

0.5°C, which was not suitable to this kind of experiment. Therefore, we tried to eliminate operator interaction with the experiment by creating a program in the Dimensional Measuring Interface Standard (PC-DMIS 2013 MR1 software). Consequently, we conducted completely automated measurements, as shown in Fig. 2.

3.3. Verification method

In our case study, the adopted version of the procedure described in ISO 10360-2 [1] was used. Experimental measurement was carried out at 52 reference points. Each of the measurements started at the center of each hole (the CMM measured all three axes of each point) and the intersection length between the hole centers. The errors measurement of the calibrated workpiece were used to determine the measurement uncertainties for the actual measurements. A calibrated workpiece is a workpiece whose dimensions are known with high accuracy. The described method utilized calibrated workpieces. Therefore, it took into account systematic measurement errors, which simplified the process of proving traceability. Metrological traceability was essential to ensure that the measurement results were repeatable, reproducible, and reliable regardless of the place where the methods and instruments were implemented. The method described above is reliable for the determination of the thermal induced measurement errors. However, it is generally costly and time consuming [5].

In the experimental part, we conducted long-term measurements. They were normally started after more than a six-hour working time of the CMM. However, short-term measurements were performed with a two-hour thermal relaxation time after each measurement. In addition, low and improved industrial environments (borrowing the terminology from ISO 230-9) were created and set. The measurements performed taken to evaluate the effect of temperature deviation as a factor in calculating the CMM errors. It should be mentioned here that we tried to replicate medium industrial environment for the LIC. Moreover, *medium environmental conditions* (MIC) were created, which was another common environment which could be applied between the LIC and the IIC. This aided our understanding of the thermal effects in a typical industry environment. The material temperature sensors were located close to the X-axis, Y-axis, and Z-axis scales and on the surface of the measurement object as Fig. 1(a) illustrates. Moreover, there was no significant discrepancy in temperature for more than five days of testing. The experimental settings for five repeated measurements are displayed in Table 1. To better understand the thermal effect on the degree of uncertainty of the measurement result of CMM, we carried out experiments with various parameters:

Table 1. Parameters of experiments (adapted with permission from [8]).

Parameters	**Low industrial conditions (ISO 230-9)**	**Long-term measurements in improved industrial conditions**	**Short-term measurements in medium industrial conditions**
Temperature range	23 ± 1.5°C	19.2 ± 0.2°C	20.5 ± 0.5°C
Measurement strategy	Before rotating the workpiece by 180°	Before rotating the workpiece by 180°	After rotating the workpiece by 180°
Average sensor measurements of temperature gradient:			
CMM structure	23 ± 0.5°C	19.2 ± 0.1°C	20.5 ± 0.45°C
Workpiece	23 ± 0.4°C	19.2 ± 0.15°C	20.5 ± 0.4°C
Probe	23 ± 0.2°C	19.2 ± 0.1°C	20.5 ± 0.4°C

Metrol. Meas. Syst., Vol. 28 (2021), No. 4, pp. 609–626
DOI: 10.24425/mms.2021.137699

3.4. Development of the measurement model

In practise, metrological laboratories deal well with time-varying temperature influence. However, with CMMs, which are installed in industrial shops, one must take into consideration the uncertainty estimation. In this context, an appropriate model equation must be developed according to the standard [27] to fit the CMM measurement of the given study. Another interesting property of proposed model functions is the temperature correction for the length measurement at 20°C included in the model. The mathematical model of the hole plate calibration is shown in (1):

$$L = L_R \left(1 + \alpha_g \cdot \theta_g + \alpha \cdot \Delta t_x - \alpha \cdot \theta\right) + 2 \cdot R \left(\alpha_g \cdot \theta_g - \alpha_p \cdot \theta_p\right) + \Delta L \left(1 - \alpha \cdot \theta\right) + L_{RP}, \quad (1)$$

where, L is the observed length of the hole plate at 20°C; L_R is the reading of the CMM at 20°C; R is the radius of the probe at 20°C; ΔL is the axial calibrated value of CMM; α, α_g, α_p are CTE of the hole plate, scale, and probe, respectively; θ, θ_g, θ_p are temperature deviations of the hole plate, scale, and probe from 20°C, respectively; L_{RP} is the correction due to the reproducibility of the probe system; Δt_x is the correction due to the temperature difference between the holes.

The measurements are repeated n times for the hole plate calibration. The uncertainty is evaluated from the observed maximum standard deviation. Since the variables θ, θ_g, and θ_p are dependent on each other, the following transformations make them independent [15].

$\delta\theta_g = \theta_g - \theta$ – temperature difference between optical scale and test item,
$\delta\alpha_g = \alpha_g - \alpha$ – CTE difference between optical scale and test item,
$\delta\theta_p = \theta_p - \theta$ – temperature difference between probe and test item,
$\delta\alpha_p = \alpha_p - \alpha$ – CTE difference between probe and test item.

The correction due to reproducibility of the probe system is denoted as Δl_{RP}. If a measurement stylus tip is used to measure the standard hole, the reproducibility of the probe system is less than x µm, which is the uncertainty component introduced by the sampling strategy and the uncertainty probability is calculated assuming the distribution is rectangular $\sqrt{3}$, and the standard uncertainty is calculated as shown in (2):

$$L_{RP} = \frac{x}{\sqrt{3}} \cdot \mu\text{m}\,. \quad (2)$$

One effective way of reducing significantly the correction due to reproducibility is using spectral analysis to identify the best sampling strategy and estimate the changes of the measurement results from the difference between the actual measurement points and the optimal sampling points to evaluate the uncertainty caused by the sampling strategy. Consequently, the influence of last parameter can be ignored when determining the number of optimal sampling points [29].

4. Measurement results

The explanation of CMM length measurement error is briefly provided, and a detailed explanation can be found in standards [1, 29]. First, measurements were performed with the use of the hole plate in three cross-sections using three points to precisely identify the midpoint of each hole using PC-DMIS. Second, the files received from the software contained coordinates (measured X,Y and Z locations) of all 52 holes of plate standard centres. Thirdly, the Pythagoras Theorem to derive a formula for finding the distance between two points in a 3-dimensional space was used. Let $A = (x_1, y_1, z_1)$ and $B = (x_2, y_2, z_2)$ be two points on the Cartesian plane. The distance

between A and B is calculated as is shown in (3).

$$AB = \sqrt{(x_2 - x_1)^2 + (y_2 - y_1)^2 + (z_2 - z_1)^2}\,. \tag{3}$$

Finally, subtraction of the calculated values of hole centre coordinates with the calibrated values by PTB was performed to estimate the error of the length measurement.

The following diagrams (Figs. 3–5) display the results of the measurements of the LIC, MIC, and IIC. Fig. 3 illustrates the measurement results under the LIC. The abscissa shows the number of sampling points and the ordinate shows the error of the CMM in μm. It shows the proof that the environmental influence on the measurement was not negligible. The dispersion of the gradient of temperature by the axes of the CMM and the workpiece could be a significant issue and it might cause such negative influence. The other pairs of diagrams illustrate the MIC and IIC measurements, which were performed short term and long term, respectively.

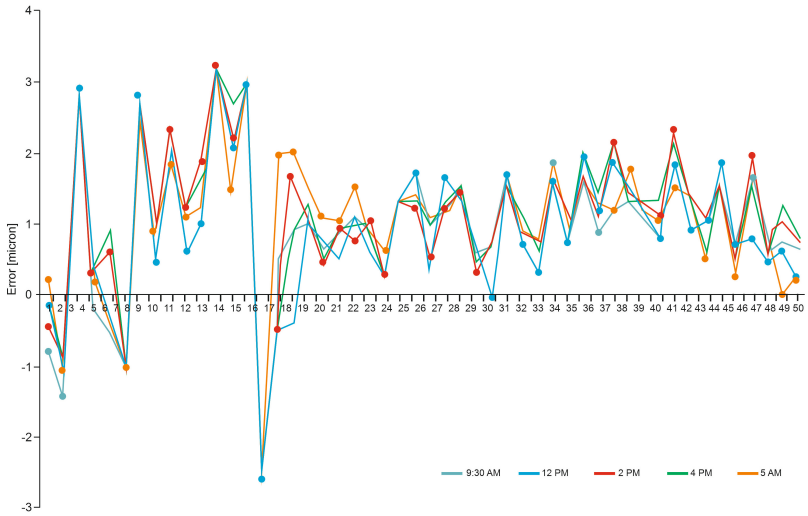

Fig. 3. Whole measurement results under low industrial conditions.

From Fig. 3, it is clear that the measurement results under the LIC lacked accuracy because almost all of the calibration point results moved to nearly 1.2 μm. It should be noted that dimensions are linked to the temperature at which they are measured. The effect of the temperature fluctuating environment influenced the hole plate and it can be determined by measuring a material standard a large number of times. Thus, it can be seen from the Fig. 3 that CMM in the LIC shows significant errors in comparison with the calibration results provided by PTB.

It is clear from Figs. 3–5 that the measurements, which were conducted under the MIC and IIC, had both precise accuracy and repeatability. However, it should be noted that first 15 minutes of the measurements still had sharp resonances. The difference curves which were obtained for each environmental condition under the IIC were identical on the micrometer level for the temperature range under consideration. They could be considered to have measurement durations which were independent for this research.

After comparing the data, the following observations were made. The difference between the errors of the LIC and IIC in coordinates was within the range of 1.2 μm. The difference between the errors of the long-term IIC and short-term MIC in coordinates was within the range of 0.2 μm.

Metrol. Meas. Syst., Vol. 28 (2021), No. 4, pp. 609–626
DOI: 10.24425/mms.2021.137699

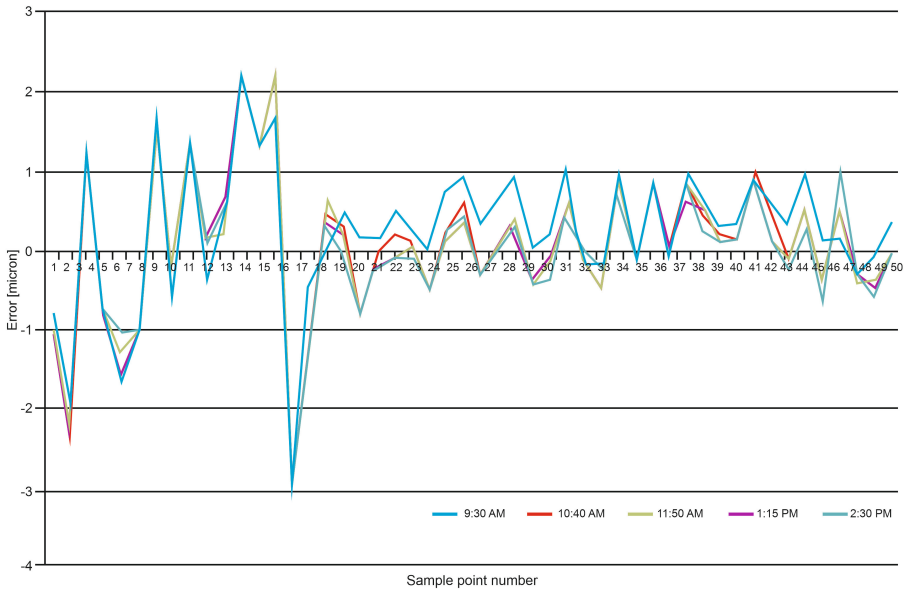

Fig. 4. Whole measurement results under MIC (short term).

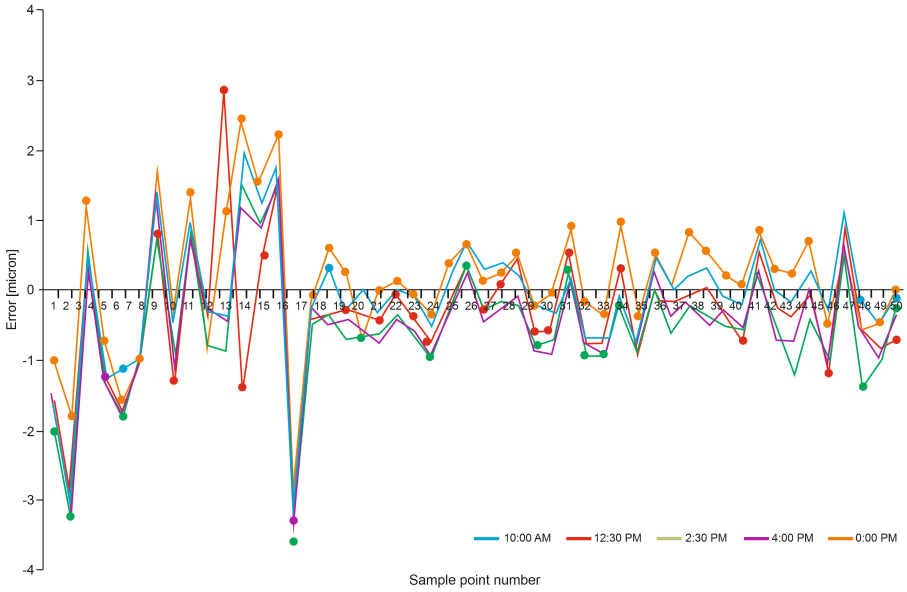

Fig. 5. Whole measurement results under IIC (long term).

The last difference was not significant due to a close temperature range with comparison between the LIC and IIC data for which all of the measurement results moved by more than 1 micrometer.

The differences for each industrial conditions are illustrated in Fig. 6, which shows the average measurement results between the LIC and IIC (long term) and the MIC (short term). In both cases

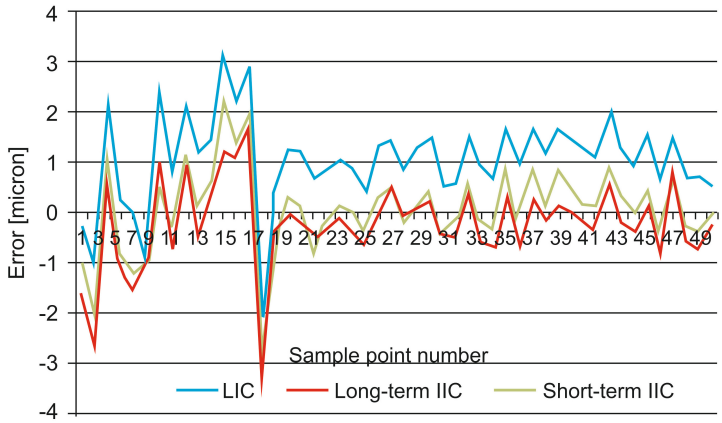

Fig. 6. Average measurement results for each industrial conditions: LIC, IIC (long term), and MIC (short term).

(IIC and MIC), the length measurement error of a CMM ($E_0 \approx 1.55$ µm) could not exceed the maximum permissible error of the CMM. Despite the fact that the MIC (short term) measurements were conducted in higher temperature ranges than the IIC (long term) measurements, the results of the MIC were almost the same as those of the IIC. The reason for this might have been the heat emission from the CMM components, which increased the error in the IIC (long term) measurement results. However, as shown by the graph, the LIC had the highest rate of error compared to the other industrial conditions.

5. Improved CMM calibration uncertainty assessment technique

There are several factors which contribute to uncertainty in measurement. Typically, the uncertainty varies depending on the workpiece being measured, the operator, and the strategy used for measurement. The measurement strategy comprises the procedure of measurement, the location of the workpiece in the CMM volume styli configuration, and the probing strategy.

An improved version of the current level in assessing this calibration and verification uncertainty was discussed, in some detail, in references [4, 28]. Task-specific experiments based on the identification of residual errors using a hole plate standard were performed, and the authors concluded that thermal fluctuations were a major source of uncertainty in the measurements. According to reference [28], the main causes of uncertainty are a) machine uncertainty, b) thermally-induced uncertainty, and c) sampling uncertainty.

The combined uncertainty, u_c, is calculated as shown in (4):

$$u_c = \sqrt{u_M^2 + u_S^2 + u_T^2}\,. \tag{4}$$

Finally, the expanded uncertainty, U, is obtained using (5):

$$U = k \times u_c\,. \tag{5}$$

5.1. CMM uncertainty

The improvement was made for CMM uncertainty calculation according to reference [28] in accordance with published standard [1, 30] which could be used for calculating the machine

Metrol. Meas. Syst., Vol. 28 (2021), No. 4, pp. 609–626
DOI: 10.24425/mms.2021.137699

uncertainty. The uncertainty component u_M was caused by the bias and linearity of the CMM dimensional measurement tasks, as shown in (6):

$$u_M = \frac{MPE_E}{\sqrt{3}} = \frac{1}{\sqrt{3}}(a + b \times L), \tag{6}$$

where L is the length being measured (in our case the distance was equal to 50 mm).

When the equation was applied to the workpiece which was measured multiple times under the same conditions, the laboratory standard deviation of a single measurement was calculated using the Bessel formula, as shown in (7):

$$S = \sqrt{\frac{1}{n-1}\sum_{j=1}^{n}(y_i - \bar{y})^2}, \tag{7}$$

where n is the number of repeated measurements, y_i is the measured value of the i^{th} measurement, and $\bar{y}$ is the average value of the repeated measurement column.

The uncertainty component, u_r, caused by the measurement repeatability of the N number of measurement meant that the best estimation was obtained with (8):

$$u_r = \frac{S}{\sqrt{N}} = \sqrt{\frac{\sum_{j=1}^{n}(y_i - \bar{y})^2}{N(n-1)}}. \tag{8}$$

When an operator carries out repeated m groups of independent measurements for every dimension of a test workpiece, the average value of a group j of repeated measurement columns should be set as y_j. Furthermore, considering the mean value y_j of the column consisting of m groups of measurements as a measurement column, one must work out the mean value y of the measurement column and the uncertainty component u_R caused by the reproducibility [28], which can be presented as shown in (9):

$$u_R = \sqrt{\frac{\sum_{j=1}^{m}(y_i - \bar{\bar{y}})^2}{(m-1)}}. \tag{9}$$

Finally, the total CMM uncertainty can be calculated as follows:

$$uu_c = \sqrt{\frac{MPE_E^2}{3} + \frac{\sum_{j=1}^{m}(y_i - \bar{y})^2}{N(n-1)} + \frac{\sum_{j=1}^{m}\left(y_i - \bar{\bar{y}}\right)^2}{(m-1)}}. \tag{10}$$

5.2. Sampling uncertainty

This contribution to the uncertainty constituted a feature and assessment of the sampling uncertainty related to the statistical sampling approach [31]. The standard deviation of a sample mean was the sum of standard deviations for each hole distance measurement of the population divided by the square root of the sample size (n) [32], as shown in (11):

$$u_S = \frac{\sigma_{apc}}{\sqrt{n-x}}, \tag{11}$$

where σ_{apc} is the average point coordinate error from five repeated measurement results, n is the number of points probed to define the feature, and x is the minimum number of points required to define a given feature ($e.g.$ $x = 2$ for a line, $x = 3$ for plane or circle, $x = 4$ for sphere, and $x = 5$ for cylinder).

5.3. Temperature-induced uncertainty

There are several contributors to the uncertainty of a nominal expansion of a part or scale. In practice, the dominant contributing factors are as follows [27]:

- uncertainty in the CTE,
- uncertainty in the temperature measuring instrument,
- variations of the temperature from its mean value.

The influences of time-dependent temperature environment on the measurement result are expressed as a component of complex standard uncertainty, the total thermal uncertainty, u_T, calculated using the formula [34]:

$$u_T = \sqrt{UNE_S^2 + UNE_W^2 + LUTM_S^2 + LUTM_W^2}\,, \tag{12}$$

where $LUTM$ is the length uncertainty due to temperature measurement, and UNE is the uncertainty of the nominal thermal expansion, calculated as

$$UNE_X = \sqrt{L^2 \times u_{\alpha_X}^2 \times (T_{X_{AVG}} - 20)^2}\,. \tag{13}$$

In (2), X is equal to S or W, characterizing scale or workpiece, respectively, L is the length, and u_{α_X} is the uncertainty associated with the CTE obtained from:

$$u_{\alpha_X} = C_D \times 0.1 \times \alpha_X\,. \tag{14}$$

where C_D is the coefficient regarding the temperature distribution (applied in order to convert the limits of variation into a standard deviation), α_X is the CTE for the scale or workpiece (such values can be obtained from a calibration certificate). The prevailing values of CD are 0.5 for normal, 0.6 for rectangular, and 0.7 for U-shaped distributions [2]. The 0.1 factor in (7) originates from the approximation that both the calibrated and published CTE have a ±10% variation.

$LUTM_X$ can be written in a final form:

$$LUTM_X = \sqrt{(L^2 \times \alpha_X^2 \times u_{TX1}^2) + (L^2 \times \alpha_X^2 \times u_{TX2}^2)}\,. \tag{15}$$

u_{TX1} is the uncertainty resulting from temperature fluctuations in the machine scale or workpiece; it is given by:

$$u_{TX1} = (T_{X\,\max} - T_{X\,\min}) \times C_D\,. \tag{16}$$

u_{TX2} is the uncertainty of the temperature-measuring instrument (used for the measuring scale or workpiece temperature), which is derived from calibration certificates provided by the manufacturer.

Based on the results obtained (Table 2), there were several inferences.

The estimated uncertainty of CMM calibration results of the proposed method was close to similar uncertainty of CMM calibration results [34], which was equal to 3.1 μm for IIC.

a) the total uncertainty of the measurement result under the LIC was higher than the uncertainties obtained under other industrial conditions;

Metrol. Meas. Syst., Vol. 28 (2021), No. 4, pp. 609–626
DOI: 10.24425/mms.2021.137699

Table 2. Uncertainty contributors for the hole plate measurement under various environmental conditions.

Source	Equation number	Result, µm under the LIC at 23.5°C	Result, µm under the MIC at 20.3°C	Result, µm under the IIC at 19.2°C
Machine				
u_M	(6)	0.9	0.9	0.9
S	(7)	0.92	0.98	0.91
u_r	(8)	0.13	0.14	0.13
u_R	(9)	0.93	0.98	0.89
uu_c	(10)	1.6	1.65	1.56
Sampling u_S	(11)	0.36	0.04	0.03
Thermal				
UNE_S	(13)	0.02	0.002	0.005
UNE_W	(13)	0.11	0.013	0.016
$LUTM_S$	(15)	0.05	0.014	0.01
$LUTM_W$	(15)	0.26	0.1	0.07
u_T	(12)	0.29	0.1	0.07
Combined uncertainty				
u_c	(4)	1.69	1.65	1.56
Expanded uncertainty				
U (k = 2)	(4)	3.4	3.3	3.1

b) the main part of the uncertainty component was associated with the CMM accuracy and the repeatability;
c) each component of the total thermal uncertainty was doubled in comparison with other environmental conditions.

Following the obtained results from both previous research [8] and current case study, it can be seen that the most influential factor in the measurement uncertainty expressed is the accuracy of the CMM parameters [35]. Disregarding the uncertainty component associated with the Maximum Permissible Indication Error ($E_{0,\,\mathrm{MPE}}$), which was mainly related to CMM errors, one could conclude that the environmental impact was the main contributing to the uncertainty, and it completely dominated the overall uncertainty budget for the given study. Additionally, the dispersion of the gradient of the temperature by the X, Y, and Z axes of the CMM and the workpiece could be a significant issue. However, other thermal influences related aspects also needed to be considered. In this regard, the best solution was to compensate for the thermal error with the control of the heat fluxes into the system. Thus, it would be possible to compensate for the error by means of the controlled relative motion in the frame [26]. Even with precise temperature-controlled rooms and compensation systems, when it came to long length calibrations, the main contributor of the uncertainty budget was still related to thermal influences of internal heat sources of the machine [13].

6. Discussion

Since CMMs consist of several components, many metrological parameters are not stable in the function of time, especially when they are measured in the temperature fluctuating environment. In practice, correction of temperature-induced errors is not an easy task to achieve. Understanding the nature of varying ambient conditions is still challenging. Most CMM users, even skilled portable metrology operators, have to consider a number of issues such as thermal influences, machine repeatability, and reproducibility, *etc.* because these factors should normally be considered in

a calibration uncertainty of the CMMs. So, there is still confusion about what may or may not be included in the uncertainty analysis. To better understand the latter issue more practical approaches should be implemented [8].

The equation presented in Section 3.4 accounts for the errors of the length measurements of a simple component. This equation seems like it would only be applicable to estimating the uncertainty of measurements in one linear direction. This model can be generalized for complex workpieces such as out-of-plane parallelism of axes curved components, workpieces composed of multiple materials, or pieces with large variations in the dimensions (*e.g.* a wedge-shaped piece which is very thick on one end and very thin on the other end).

The thermal influences have a complex nature. It is difficult to manage the thermal expansion of measurement object simply assuming that dimensional changes would be "linear". In practice, in the real world, the operators came across not only a specific material but different combinations of materials. Therefore it is not universally applicable to compensate for CTE. Consequently, it should be taken into consideration that the temperature induced uncertainty applied in this research has a limitation and only applicable for homogeneous materials. Finally, the best practice for specific measurement task is to determine a suitable method by implementing several compensation techniques. Alternatively, there are several software packages to manage temperature compensation. For instance, the temperature of the measurement object can be measured at several points during a measuring cycle and stored in the measuring system with an appropriate compensation tool for the CTE. In addition, it should be noted that a temperature-controlled room and use of additional temperature sensors for better environmental control seems to be advantageous for the most accurate measurements.

Consequently, the authors believe that it would be valuable to repeat the experiment described in this research on a variety of high-precision machines to improve compensation techniques for temperature-induced uncertainties. Furthermore, more features, measurement objects, and different sizes should be investigated.

7. Conclusions

This research presents the uncertainty estimation for a very specific measuring task, where the time-varying temperature environment must be considered, as it influences the uncertainty of CMM calibration. The influence of the last was investigated by measuring the calibration object multiple times in both different orientations in the CMM measurement range and in temperature fluctuating environment. There was a noticeable effect on the measurement results as the errors of the CMM in the LIC were greater the further away from the IIC temperature range, as predicted. It was determined that the temperature induced uncertainty had a significant effect on the uncertainty budget next to the accuracy of the CMM.

The proposed improved uncertainty assessment technique was suitable for the estimation of calibration uncertainty of the CMM in this study by properly taking into account thermal influences. The main issues for the calibration uncertainty of Coordinate Metrology were discussed, and some specific points were identified for further improvement. The solution, as the calibration uncertainty technique, was given to fulfill a number of issues related to the time-varying temperature environment and machine repeatability which would normally be considered in a calibration uncertainty analysis. For the CMM with a measurement range from 0 to 50 mm, the estimated expanded uncertainty was 3.1 μm with a coverage factor of 1.98 at a confidence level of approximately 95%.

The proper estimation of the calibration uncertainty of the CMM is important. Because if it could be reduced, it will help decrease the measurement uncertainty of the CMM. The case study

Metrol. Meas. Syst., Vol. 28 (2021), No. 4, pp. 609–626
DOI: 10.24425/mms.2021.137699

results shows that measurement uncertainty can be reduced, if we use a high precision instrument such as laser interferometer. The proposed technique was experimentally proved in the technical base of the National Scientific Centre – "Institute of Metrology", Ukraine.

Thermal contributions to the overall performance of a CMM can be the single most influential part of the error budget. Additionally, the performance of the precision of a CMM is often dictated by its thermal stability. The main reason for this is the number of different materials and interfaces found in a mechanical design. The mechanical properties of independent materials such as thermal expansion coeffcients and mechanical joints can cause stress distributions to arise as a system reacts to thermal changes. That is why the mechanism to distort, grow, or contract with the temperature changes with time [26].

An analysis of the calibration of the CMM dependent upon the ambient thermal environment in which it operated was attempted. Temperature fluctuations can lead to expansion, contraction, and deformation of the measured machine's structure, scales, and artifacts in a non-linear manner. The change in the environment (including internal heat sources of the CMM) can cause changes in the thermal field of the object of measurement. The change in the thermal field state is related to internal material stresses which cause dimensional deformation in the body of the calibration object. Any change of the heat transfer state affecting the measured object will create changes in the thermal field within its components, thus causing them to vary from its nominal dimensions, as defined during the calibration process [24]. These thermally induced changes can lead to significant measurement errors, which must be compensated for in various ways. It is critical that the approach to estimating uncertainty is well defined and unilaterally applied. This is especially true in the context of measurements in workshops where temperature is difficult to control.

Eliminating thermal errors can be one of the most difficult aspects of any precision design. It should be noted that there are three general mechanisms [10] for heat transfer which are all relevant to precision machine design. A thermal error can be considered a systematic error which can be corrected, while temperatures are recorded and used by the software. However, this is an (unknown) bias error in the case of a correction system incompatible with thermometer data.

The uncertainty while calibrating and testing an instrument now has a weight equal to the actual measured errors of the instrument. Just as metrology companies presently compete in product specifications, ISO 14253-1 demands competition in the area of uncertainty. Competition in this area with poor understanding and lack of generally accepted practice may lead to unclear results. In addition, uncertainties have not always been particularly small when compared to product tolerances. Therefore, the industry may observe an increase in the level of tolerances or more difficult tasks to comply with current tolerances.

Acknowledgements

This research was funded by the National Natural Science Foundation of China (grant number 51765012). Special thanks to Alex Leonidovich Kostrikov – the National Scientific Centre "Institute of Metrology", Ukraine and Gulsim Rysbayeva – a Ph.D. student at Guilin University of Electronic Technology, China for their kind help in performing experimental part of this research and many helpful suggestions.

References

[1] International Organization for Standardization (2009). *Geometrical product specifications (GPS) – Acceptance and reverification tests for coordinate measuring machines (CMM) – Part 2: CMMs used for measuring linear dimensions* (ISO Standard No. 10360-2:2009). https://www.iso.org/standard/40954.html

[2] International Organization for Standardization (2017). *Geometrical product specifications (GPS) – Inspection by measurement of workpieces and measuring equipment – Part 1: Decision rules for proving conformance or non-conformance with specifications* (ISO Standard No. 14253-1:2017). https://www.iso.org/standard/70137.html

[3] Mussatayev, M., Huang, M., & Tang, Zh., (2020). Current issues in uncertainty of dimensional tolerance metrology and the future development in the domain of tolerancing. *IOP Conference Series: Materials Science and Engineering*, *715*(1). https://doi.org/10.1088/1757-899X/715/1/012084

[4] Leach, R., & Smith, S. T. (Eds.). (2018). *Basics of Precision Engineering*. CRC Press.

[5] David, F., & Hannaford, J. (2012). *Good Practice Guide No. 80*. National Physical Laboratory.

[6] International Organization for Standardization (2013). *Geometrical product specifications (GPS) – Coordinate measuring machines (CMM): Technique for determining the uncertainty of measurement – Part 1: Overview and metrological characteristics* (ISO Standard No. ISO/TS 15530-1). https://www.iso.org/standard/38693.html

[7] Płowucha, W. (2019). Point-straight line distance as model for uncertainty evaluation of coordinate measurement. *Measurement*, *135*, 83–95. https://doi.org/10.1016/j.measurement.2018.11.008

[8] Mussatayev, M., Huang, M., & Beshleyev, S. (2020). Thermal influences as an uncertainty contributor of the coordinate measuring machine (CMM). *The International Journal of Advanced Manufacturing Technology*, *111*, pp. 537–547. https://doi.org/10.1007/s00170-020-06012-3

[9] Sładek, J., & Gąska, A. (2012). Evaluation of coordinate measurement uncertainty with use of virtual machine model based on Monte Carlo method. *Measurement*, *45*(6), 1564–1575. https://doi.org/10.1016/j.measurement.2012.02.020

[10] Saunders, P., Verma, M., Orchard, N., & Maropoulos, P. (2013). The application of uncertainty evaluating software for the utilisation of machine tool systems for final inspection. *10th International Conference and Exhibition on Laser Metrology, Coordinate Measuring Machine and Machine Tool Performance, LAMDAMAP 2013*, 219–228.

[11] International Organization for Standardization (2011). *Geometrical product specifications (GPS) – Coordinate measuring machines (CMM): Technique for determining the uncertainty of measurement – Part 3: Use of calibrated workpieces or measurement standards* (ISO Standard No. 15530-3). https://www.iso.org/standard/53627.html

[12] International Organization for Standardization (2004). *Geometrical Product Specifications (GPS) – Coordinate measuring machines (CMM): Technique for determining the uncertainty of measurement – Part 3: Use of calibrated workpieces or standards* (ISO Standard No. ISO/TS 15530-3). https://www.iso.org/standard/38695.html

[13] European Cooperation for Accreditation of Laboratories. (1995). Coordinate Measuring Machine Calibration [Publication Reference, EAL-G17].

[14] International Organization for Standardization. (2006). *Geometrical product specifications (GPS) – Guidelines for the evaluation of coordinate measuring machine (CMM) test uncertainty* (ISO Standard No. ISO/TS 23165). https://www.iso.org/standard/24236.html

[15] Fang, C. Y., Sung, C. K., & Lui, K. W. (2005). Measurement uncertainty analysis of CMM with ISO GUM. *ASPE Proceedings*, United States, 1758–1761.

[16] Płowucha, W. (2020). Point plane distances model for uncertainty evaluation of coordinate measurement. *Metrology and Measurement Systems*, *27*(4), 625–639. https://doi.org/10.24425/mms.2020.134843

[17] Ruffa, S., Panciani, G. D., Ricci, F., & Vicario, G. (2013). Assessing measurement uncertainty in CMM measurements: comparison of different approaches. *International Journal of Metrology and Quality Engineering*, *4*(3), 163–168. https://doi.org/10.1051/ijmqe/2013057

Metrol. Meas. Syst., Vol. 28 (2021), No. 4, pp. 609–626
DOI: 10.24425/mms.2021.137699

[18] Cheng Y. B., Chen X. H., & Li Y. R. (2020). Uncertainty Analysis and Evaluation of Form Measurement Task for CMM. *Acta Metrologica Sinica*, *41*(2), 134–138. https://doi.org/10.3969/j.issn.1000-1158.2020.02.02 (in Chinese).

[19] Rost, K., Wendt, K., & Härtig, F. (2016). Evaluating a task-specific measurement uncertainty for gear measuring instruments via Monte Carlo simulation. *Precision Engineering*, *44*, 220–230. https://doi.org/10.1016/j.precisioneng.2016.01.001

[20] Valdez, M. O., & Morse, E. P. (2017). The role of extrinsic factors in industrial task-specific uncertainty. *Precision Engineering*, *49*, 78–84. https://doi.org/10.1016/j.precisioneng.2017.01.013

[21] Yang, J., Li, G., Wu, B., Gong, J., Wang, J., & Zhang, M. (2015). Efficient methods for evaluating task-specific uncertainty in laser-tracking measurement. *MAPAN-Journal Metrology Society of India*, *30*(2), 105–117. https://doi.org/10.1007/s12647-014-0126-9

[22] Haitjema, H. (2019). Calibration of displacement laser interferometer systems for industrial metrology. *Sensors*, *19*(19), 4100. https://doi.org/10.3390/s19194100

[23] Doytchinov, I., Shore, P., Nicquevert, B., Tonnellier, X., Heather, A., & Modena, M. (2019). Thermal effects compensation and associated uncertainty for large magnet assembly precision alignment. *Precision Engineering*, *59*, 134–149. https://doi.org/10.1016/j.precisioneng.2019.06.005

[24] Van Gestel, N. (2011). *Determining measurement uncertainties of feature measurements on CMMs (Bepalen van meetonzekerheden bij het meten van vormelementen met CMMs)* [Doctoral dissertation, Katholieke Universiteit Leuven]. Digital repository for KU Leuven Association. https://lirias.kuleuven.be/retrieve/157334

[25] Mussatayev, M., Huang, M., & Rysbayeva, G. (2019). Role of uncertainty calculation in dimensional metrology using Coordinate Measuring Machine. *ARCTIC Journal*, *72*(6).

[26] International Organization for Standardization (2005). Test code for machine tools – Part 9: Estimation of measurement uncertainty for machine tool tests according to series ISO 230, basic equations (ISO Standard No. ISO/TR 230-9:2005). https://www.iso.org/standard/39165.html

[27] International Organization for Standardization (2008). Uncertainty of measurement-Part 3: Guide to the expression of uncertainty in measurement (GUM: 1995). https://www.iso.org/standard/50461.html

[28] Cheng, Y., Wang, Z., Chen, X., Li, Y., Li, H., Li, H., & Wang, H. (2019). Evaluation and optimization of task-oriented measurement uncertainty for coordinate measuring machines based on geometrical product specifications. *Applied Sciences*, *9*(1), 6. https://doi.org/10.3390/app9010006

[29] Jakubiec W., & Płowucha W. (2013). First Coordinate Measurements Uncertainty Evaluation Software Fully Consistent with the GPS Philosophy. *Procedia CIRP*, *10*, 317–322. https://doi.org/10.1016/j.procir.2013.08.049

[30] International Organization for Standardization. (2013). *Geometrical Product Specifications (GPS) – systematic errors and contributions to measurement uncertainty of length measurement due to thermal influences* (ISO Standard No. ISO/TR 16015:2003). https://www.iso.org/standard/29436.html

[31] Huang, Z., Zhao, L., Li, K., Wang, H., & Zhou, T. (2019). A sampling method based on improved firefly algorithm for profile measurement of aviation engine blade. *Metrology and Measurement Systems*, *26*(4), 757–771. https://doi.org/10.24425/mms.2019.130565

[32] Ramesh, R., Mannan, M. A., & Poo, A. N. (2000). Error compensation in machine tools. A review: part I: geometric, cutting-force induced and fixture-dependent errors. *International Journal of Machine Tools and Manufacture*, *40*(9), 1235–1256. https://doi.org/10.1016/S0890-6955(00)00009-2

[33] International Organization for Standardization. (2004). *Test conditions for numerically controlled turning machines and turning centres – Part 8: Evaluation of thermal distortions* (ISO Standard No. ISO 13041-8:2004). https://www.iso.org/standard/34663.html

[34] Doytchinov, I., (2017). Alignment measurements uncertainties for large assemblies using probabilistic analysis techniques. [Doctoral dissertation, Cranfield University]. CERN Document Server. https://cds.cern.ch/record/2299206

[35] Štrbac, B., Radlovački, V., Spasić-Jokić, V., Delić, M., & Hadžistević, M. (2017). The difference between GUM and ISO/TC 15530-3 method to evaluate the measurement uncertainty of flatness by a CMM. *MAPAN*, *32*(4), 251–257. https://doi.org/10.1007/s12647-017-0227-3

Meirbek Mussatayev is a Ph.D. candidate of Guilin University of Electronic Technology, China. He obtained the B.Sc. and M.Sc. degrees in Automation and Control and Mechanical Engineering from Kazakh Academy of Transport and Communications, Kazakhstan and Tomsk Polytechnical University, Russia in 2009 and 2013, respectively. His research activity focuses on Dimensional Metrology.

Meifa Huang is currently a professor at School of Electrical and Mechanical Engineering, Guilin University of Electronic Technology, China. He received his Ph.D. in Mechanical Manufacture and Automation from Huazhong University of Science and Technology in 2004, and he has published over 100 papers, including 53 papers indexed by SCI or EI. His main research interests are computer-aided tolerancing, precision design of mechatronic systems and intelligent measurement method.

Marat Nurtas is assistant professor of the Department of Mathematical and Computer Modeling, International Information Technologies University, Kazakhstan. He obtained the B.Sc. in Mathematics from Al-Farabi Kazakh National University, and the Ph.D. in Mathematical and Computer Modeling, KBTU, Kazakhstan.

Azamat Arynov is a research student (EngD) at School of Engineering, University of Warwick, UK. He obtained the B.Sc. from Almaty University of Power Engineering and Telecommunications, Kazakhstan and M.Sc. degree in Electrical Engineering, from Newcastle University, UK in 2008 and 2013, respectively.